Migration of population to higher-angular-momentum Rydberg states through the degenerate Raman coupling

Rainer Grobe,* Gerd Leuchs,† and Kazimierz Rzążewski‡
Joint Institute for Laboratory Astrophysics, University of Colorado and National Bureau of Standards, Boulder, Colorado 80309
(Received 15 July 1985)

We formulate a model describing migration of population from low-l to higher-l states of the same principal quantum number in the highly excited state of the atom. The physical mechanism is the degenerate, nearly resonant Raman coupling. Specific calculations are performed for the hydrogen atom. The laser light is modeled as a monochromatic coherent or chaotic colored noise.

I. INTRODUCTION

A variety of nonlinear effects have been found in photoionization of atoms with high-intensity laser radiation.[1] If two or more photons are required to reach the continuum one inevitably deals with a multiphoton process. But even when the continuum can be reached by absorption of one photon only, additional photons may be absorbed in continuum-continuum transitions. Recent experimental results in this field[2] have prompted interesting theoretical model studies. If, on the other hand, the laser intensity is low enough so that no continuum-continuum transitions occur, the only intensity dependence left is depletion of the bound state.

It has been found,[3] however, that yet another nonlinear process can be important in the regime where only depletion is expected. In these experiments,[3] the angular distribution of the photoelectrons was measured for various laser intensities. Drastic changes of the distribution were found in cases when the initially populated bound state was nearly degenerate with one or more neighboring bound states. These results are explained by a Raman-type coupling which mixes the initially populated state with the nearby states. When the laser intensity increases, the third-order process (two-photon Raman coupling and subsequent photoionization) competes more and more effectively with the direct first-order process. In the experiment, such an intensity dependence was found, for example, in photionization from a selectively populated Rydberg *nd* state of sodium which is nearly degenerate with a whole manifold of states with different angular-momentum quantum numbers l.

In the following sections a model calculation is developed to obtain a qualitative picture of the dynamical behavior of the system. It is found that under favorable conditions the population migrates periodically from low- to high-angular-momentum states and back. One remarkable result is that in the case of a monochromatic laser, the laser intensity changes only the time scale and does not affect the characteristic of the temporal evolution.

Experimentally the predictions of this model calculation can be tested by measuring the angular distribution of photoelectrons. However, the photoionization cross section decreases strongly with increasing orbital angular-momentum quantum number l. Therefore, it may be advantageous to use field ionization—separated from the laser interaction in time or space—as a probe for the population of different l states. This can be achieved unambiguously, if the l states are not degenerate. The l degeneracy is lifted by the relativistic interactions and by the polarizability of the ionic core[4] for hydrogen and alkali-metal atoms respectively. If the electric field is then switched on slowly enough the l states will evolve adiabatically into different parabolic quantum number states which in turn have their own characteristic thresholds for field ionization.[5] As long as the interaction time between the laser pulse and the atoms is short enough, the l-state splitting can be neglected in the calculation.

Our paper is organized as follows. Basic dynamical equations of the model are derived in Sec. II. Section III is devoted to an analytically soluble example of the dynamics. In Sec. IV the actual values of ac Stark shifts, Raman couplings, and ionization rates are discussed for the highly excited state of the hydrogen atom. It is shown there that only nearly resonant Raman coupling can be strong enough to produce an effective migration of the population. Some constraints on the laser intensity, interaction time, and the detuning, required by the consistency of our model, are also discussed in Sec. IV. The averaging over chaotic, colored stochastic processes representing the multimode laser is explained in Sec. V.

Section VI contains our main numerical results. They are obtained for the Rydberg state of hydrogen atoms with principal quantum number $N=28$, irradiated by a CO_2 laser operating with an intensity of only 25 W/cm^2. The results for a monochromatic coherent field are compared with those of a chaotic colored light. A quasi-steady-state distribution of population is found if the chaotic light has a very narrow bandwidth.

II. THE MODEL

In this section we present a brief derivation of the dynamical model proposed in this paper. We have in mind highly excited states. For all the atoms they tend to have properties similar to those of the hydrogen atom. The specific calculations of our paper are done for the hy-

drogen atom, hence, we assume from the outset an exact degeneracy with regard to the angular-momentum quantum number l. The assumption is good for heavier atoms if the laser-induced level shifts (ac Stark shifts) are larger than the splitting of different l states.

Due to the electric dipole selection rules, the two-photon Raman coupling will link states with $\Delta l=2$. Hence, if the initial excitation process would produce pure, say $l=1$ state, the evolution will be confined to the manifold of odd-l states. With the assumption of linear polarization, the magnetic quantum number m will not be changed and will be suppressed in our notation. The specific calculations are done for $m=0$ hydrogenic states.

The level structure of our model atom is depicted in Fig. 1. The population is initially in the state denoted by $|1\rangle$. A general form of the state vector is

$$\psi(t)=e^{-iE_N t}\left[\sum_{j=1}\alpha_j(t)|j\rangle+e^{i\omega_L t}\sum_{j=0}\xi_j(t)|\tilde{j}\rangle + e^{-i\omega_L t}\sum_{j=0}\int\beta_j(\epsilon,t)|\epsilon,j\rangle d\epsilon\right]. \quad (2.1)$$

Taking into account the dipole coupling constants as marked in Fig. 1, the time-dependent Schrödinger equation breaks into the following set of first-order integro-differential equations for the amplitudes $\alpha_j,\xi_j,\beta_j(\epsilon)$:

$$i\dot{\alpha}_j=\int\Omega_{j-1}(\epsilon)\beta_{j-1}(\epsilon,t)d\epsilon + \int\Lambda_j(\epsilon)\beta_j(\epsilon,t)d\epsilon+\lambda_j^*\xi_j+\mu_j^*\xi_{j-1}\,, \quad (2.2a)$$

$$i\dot{\xi}_j=\lambda_j\alpha_j+\mu_{j+1}\alpha_{j+1}+\Delta\xi_j,\quad \Delta=\omega_L-(E_N-E_n)\,, \quad (2.2b)$$

$$i\dot{\beta}_j(\epsilon,t)=(\epsilon-E_n-\omega_L)\beta_j(\epsilon,t)+\Omega_j^*(\epsilon)\alpha_{j+1}+\Lambda_j^*\alpha_j\,. \quad (2.2c)$$

As is customary in the discussion of Raman coupling, we assume that the detuning Δ is large enough to make $|\tilde{j}\rangle$ states virtual. The population $|\xi_j|^2$ of these states should be negligible and we can drop a time derivative in Eq. (2.2b) eliminating ξ_j adiabatically:

$$\xi_j=-\frac{\lambda_j}{\Delta}\alpha_j-\frac{\mu_{j+1}}{\Delta}\alpha_{j+1}\,. \quad (2.3)$$

As the next step, we assume that the absorption of a single photon from the states $|j\rangle$ leads to a continuum well above the threshold. The continuum there can be regarded as nearly flat. Therefore, the continua $\beta_j(\epsilon,t)$ can be eliminated with the help of the so-called single-pole approximation.[6] The resulting set of equations takes the form

$$i\dot{\alpha}_j=\tilde{A}_j\alpha_j+\tilde{B}_j\alpha_{j-1}+\tilde{B}_{j+1}\alpha_{j+1}\,, \quad (2.4)$$

where coupling constants $\tilde{A}_j$ and $\tilde{B}_j$ are given by

$$\tilde{A}_j=-\left[\frac{|\lambda_j|^2+|\mu_j|^2}{\Delta} + \int_0^\infty\frac{|\Omega_{j-1}(\epsilon)|^2+|\Lambda_j(\epsilon)|^2 d\epsilon}{\epsilon-E_N-\omega_L}\right] -i\pi[|\Omega_{j-1}(E_N+\omega_L)|^2+|\Lambda_j(E_N+\omega_L)|^2], \quad (2.5a)$$

$$\tilde{B}_j=-\left[\frac{\lambda_j\mu_{j+1}^*}{\Delta}+\int_0^\infty\frac{\Lambda_j(\epsilon)\Omega_i^*(\epsilon)d\epsilon}{\epsilon-E_N-\omega_L}\right] -i\pi\Lambda_j(E_N+\omega_L)\Omega_j^*(E_N+\omega_L)\,. \quad (2.5b)$$

It is clear that all of the couplings $\tilde{A}_j$ and $\tilde{B}_j$ are proportional to the intensity of the electric field $|E(t)|^2$. Of course, the real part of $\tilde{A}_j$ is a light-induced shift of the level $|j\rangle$. Its imaginary part is one-half the Fermi golden rule ionization rate of that level. Parameters $\tilde{B}_j$ determine the strength of the Raman coupling.

Of course, our model atom with only one set of the nearly resonant $|\tilde{j}\rangle$ states is an oversimplification. In-

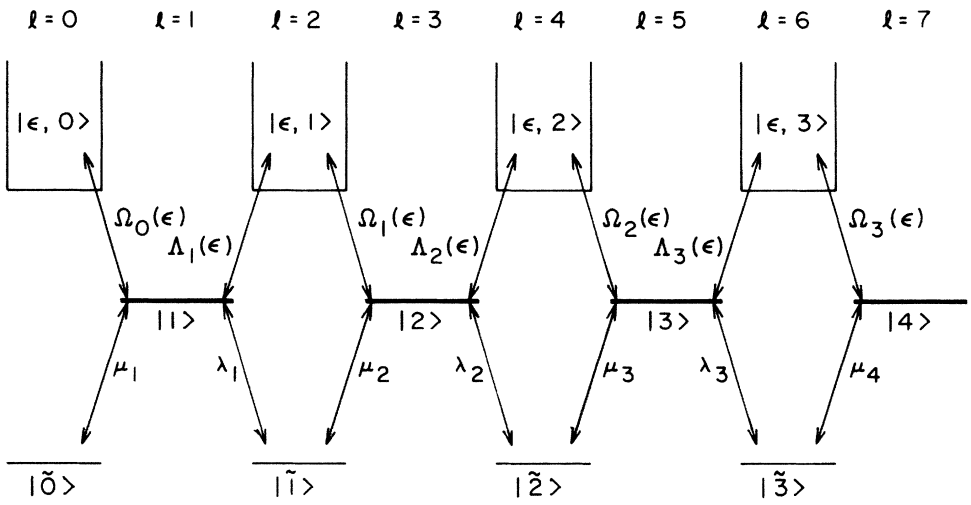

FIG. 1. Level scheme of our model atom.

clusion of other states results with sums replacing the single terms for the real parts of $\tilde{A}_j$ and $\tilde{B}_j$. Once we include, however, the contributions of far-off-resonant states, the rotating-wave approximation used so far is no longer justified and the contribution of the counter-rotating terms must be included. Of course, these contributions are obtained by a simple substitution, $\omega_L \rightarrow -\omega_L$.

This leads to the set of dynamical equations in its final form,

$$i\dot{\alpha}_j = |E(t)|^2(A_j\alpha_j + B_{j-1}\alpha_{j-1} + B_j\alpha_{j+1}) , \tag{2.6}$$

where the constants A_j and B_j are given by the following atomic matrix elements:

$$A_j = \sum_{n'l'} \left[\frac{1}{E_N - E_{n'} - \omega_L} + \frac{1}{E_N - E_{n'} + \omega_L} \right] |\langle N,2j-1 \,|\, z \,|\, n'l' \rangle|^2$$
$$- i\pi(|\langle N,2j-1 \,|\, z \,|\, E_N + \omega_L, 2j-2 \rangle|^2 + |\langle N,2j-1 \,|\, z \,|\, E_N + \omega_L, 2j \rangle|^2) , \tag{2.7a}$$

$$B_j = \sum_{n'l'} \left[\frac{1}{E_N - E_{n'} - \omega_L} + \frac{1}{E_N - E_{n'} + \omega_L} \right] \langle N,2j-1 \,|\, z \,|\, n'l' \rangle \langle n',l' \,|\, z \,|\, N,2j+1 \rangle$$
$$- i\pi \langle N,2j-1 \,|\, z \,|\, E_N + \omega_L, 2j \rangle \langle E_N + \omega_L, 2j \,|\, z \,|\, N,2j+1 \rangle . \tag{2.7b}$$

The sums $\sum_{n'l'}$ are extended over both the discrete and continuous spectrum of the atom.

Note that, due to a simple linear dependence on the laser intensity $|E(t)|^2$ of our dynamical equation (2.6), the solutions depend only on $\int_0^t |E(\tau)|^2 d\tau$ or the total energy of the laser pulse. There are no coherent pulse-shape effects in the model.

III. THE ANALYTICALLY SOLUBLE EXAMPLE

Dynamical equations, like our Eq. (2.6), linking the nearest neighbors appear very often in physics. A well-known example in optics is that of the nearly resonant multiphoton excitation of multilevel atoms.[7] For a number of specific sets of constants entering the equations, the solution can be written in a closed form.

As an illustration, we present here the simplest example. Let all the diagonal elements of the tridiagonal matrix be equal: $A_j \equiv A$ for all j, and all the off-diagonal elements are equal and real, $B_j \equiv B$.

The natural variable replacing time is

$$\eta = \int_0^t |E(\tau)|^2 d\tau . \tag{3.1}$$

Taking the Laplace transform of (2.5) with respect to η, we see that our equations take a matrix form:

$$(iz\hat{I} - \hat{A})\tilde{\alpha}(z) = i\alpha(0) , \tag{3.2}$$

where matrix $\hat{A}$ is given as

$$\begin{vmatrix} A & B & 0 & 0 & & 0 \\ B & A & B & 0 & & 0 \\ 0 & B & A & B & & 0 \\ 0 & 0 & B & A & & 0 \\ & & & & \ddots & B \\ 0 & 0 & 0 & 0 & B & A \end{vmatrix} \tag{3.3}$$

and the initial condition

$$\alpha(0) = \begin{vmatrix} 1 \\ 0 \\ 0 \\ \vdots \\ 0 \end{vmatrix} . \tag{3.4}$$

The solution of this set is

$$\tilde{\alpha}_j(z) = i\frac{1}{B}\frac{\sin[(M-j+1)\phi]}{\sin[(M+1)\phi]} , \tag{3.5}$$

where

$$iz - A = 2|B|\cos\phi \tag{3.6}$$

and M is a number of levels (dimensionality of our set).

Of course, the zeros of the denominator determine the eigenvalues of our problem or the poles contributing to the inverse Laplace transform. They are given by

$$\phi_n = \frac{n\pi}{M+1}, \quad n = 1, \ldots, M . \tag{3.7}$$

Going back to the $\eta = \int_0^t |E|^2 d\tau$ domain, we see that

$$\alpha_j(\eta) = \sum_{n=1}^{M} \left. \frac{d\tilde{\alpha}_j(z)}{dz} \right|_{z=z(\phi_n)} e^{z(\phi_n)\eta} \tag{3.8}$$

or

$$\alpha_j(t) = \frac{2e^{-iA\eta(t)}}{N+1} \times \sum_{n=1}^{M} (-1)^n \sin\left[\frac{(M-j+1)}{M+1}n\pi\right] \sin\left[\frac{n\pi}{M+1}\right] \times \exp\left\{-2i\left[|B|\cos\left[\frac{n\pi}{M+1}\right]\right]\eta\right\} . \tag{3.9}$$

Of course, one easily gets $P_j(t)=|\alpha_j|^2$, the probability of being in the jth state, out of this expression. The evolution describes an oscillatory behavior of the system.

We use this solution to illustrate a simple, although not always recognized, fact. It is clear that in spite of describing only near-neighbor interaction, matrix $\hat{A}$ in (3.3) has completely delocalized eigenvectors. All of the eigenvalues contribute to (3.9). Nevertheless, short-time behavior will be restricted to the first several levels and will not depend on the total number of levels M. This point is illustrated in Fig. 2. The population in levels 1–6 is plotted for total number of levels $M=8$ and 10.

IV. DISCUSSION OF ATOMIC PARAMETERS

In Sec. III we discussed an analytically soluble model with equal coupling constants. We devote this section to the determination of more realistic atomic parameters, using well-known hydrogenic dipole matrix elements.[8] The complex Stark shift constants A_j and Raman coupling constants B_j are given by an infinite summation over weighted dipole matrix elements from the Rydberg state with the principal number N to all possible discrete and continuum states (2.6):

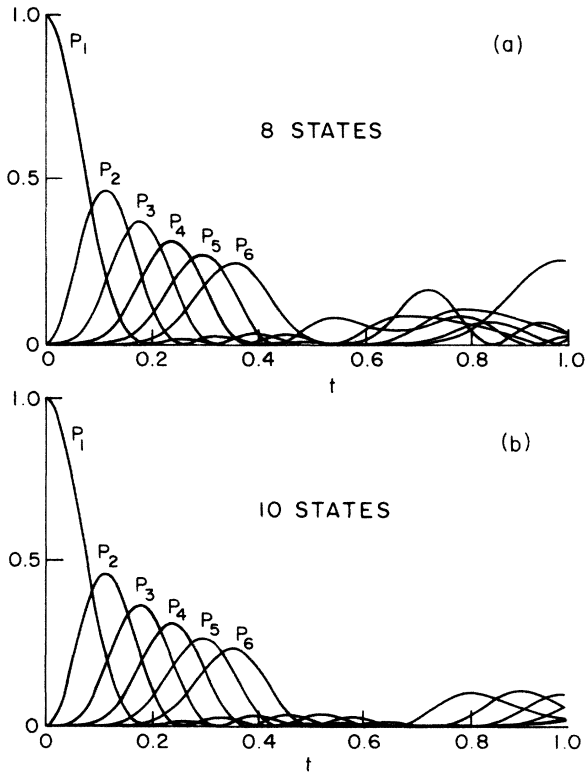

FIG. 2. Time evolution of Rydberg-state populations P_j ($j=1$–6) for the analytically soluble model with l-independent couplings. A half of the ionization rate $-\mathrm{Im}A=\frac{1}{2}$ and the Raman coupling $B=20$. (a) 8 levels, (b) 10 levels. Note that the initial phase of the evolution is the same. The solution does not depend on the ac Stark shift $\mathrm{Re}A$.

$$\mathrm{Re}A_j=\sum_{n'l'} W(n')\,|\langle N,2j-1\,|\,z\,|\,n'l'\rangle|^2\,, \tag{4.1a}$$

$$\mathrm{Re}B_j=\sum_{n'l'} W(n')\langle N,2j-1\,|\,z\,|\,n'l'\rangle\langle n'l'\,|\,z\,|\,N,2j+1\rangle\,, \tag{4.1b}$$

where the weighting function including counter-rotating terms is given by the expression

$$W(n')=\frac{2\omega_{Nn'}}{\omega_{Nn'}^2-\omega_L^2},\quad \omega_{Nn'}=E_N-E_{n'}\,. \tag{4.2}$$

The imaginary parts of the constants A_j and B_j in (2.6) can be computed directly. There are no sums over intermediate states there. In the following we have to distinguish between off-resonant (a) and near-resonant (b) cases.

(a) We consider a high-intensity Nd:YAG laser (where YAG denotes yttrium aluminum garnet), which would take the $N=30$ level of the hydrogen atom midway between the levels $n'=3$ and 4. Even though the weight function $W(n')$ has a zero for $n'=N$, major contributions to the sum come from the near vicinity of $n'=N$ because matrix elements between high-n states are orders of magnitude bigger than those between high- and low-n states. But the sign change of $W(n')$ at $n'=N$ leads to cancellations of large terms. The lowest term in a Taylor series around $n'=N$

$$W(n')=-\frac{2\omega_{Nn'}}{\omega_L^2}-\frac{2\omega_{Nn'}^3}{\omega_L^4}-\frac{2\omega_{Nn'}^5}{\omega_L^6}+\cdots \tag{4.3}$$

shows already important features. An analytical summation over the first-order weight function gives

$$\sum_{n'l'}-\frac{2\omega_{Nn'}}{\omega_L^2}\langle a\,|\,z\,|\,n'l'\rangle\langle n'l'\,|\,z\,|\,b\rangle=\frac{1}{\omega_L^2}\langle a\,|\,b\rangle\,. \tag{4.4}$$

This relation can be easily derived by evaluating the matrix element of the unit operator $[z,[H,z]]$ between the states a and b. Orthonormality of the states a and b leads to a vanishing first-order term for the Raman constants, whereas the first-order term for the Stark shift[9] (here $|a\rangle=|b\rangle$) is $1/\omega_L^2$ (≈ 545 a.u. in our case) and independent of N, as discussed by Avan *et al.*[10] Higher-order terms, for which sum rules are also derivable, have to be handled with care because of the asymptotic character of the expansion. These analytical results are in very good agreement with our numerical results, which show that the Stark shift differs from $1/\omega_L^2$ by only a few percent, whereas the Raman couplings are very small [10^{-2} (10^{-8}) a.u. for low (high) l].[11] Note, however, that the time evolution of our populations depends only on the differences between ac Stark shifts of various levels. Note that in the equal-coupling case discussed in Sec. III, the ac Stark shift enters via the overall phase factor in formula (3.9) and hence does not affect the probabilities. A considerable numerical effort is needed to determine ac Stark shifts with sufficient accuracy. The smallness of Raman couplings, however, leads us to the conclusion that even for high-power lasers such as Nd:YAG, a nonresonant electron migration to higher-l states is not feasible.

(b) For our example of near-resonant behavior we chose

transitions between $N=28$ and $n'=10$ corresponding to the wavelength of a CO_2 laser. A detuning of $\Delta=10^6-10^{-8}$ a.u. between these states makes this transition very dominant and so Stark shift and Raman coupling become comparable. For a detuning of $\Delta=5\times10^{-7}$ (≈1.2 nm) the contributions of all remaining states but $n=10$ are given by only a few percent. Surprisingly, one-fifth of the remaining contributions comes from coupling to the continuum states. The cw CO_2 laser with its high intensity and tunability corresponding to transitions between $n=10$ and $N=26$–29 is a very suitable tool to make the migration efficient.

The laser intensity, interaction time, and laser width have to obey the following constraints to make our model valid.

(a) *Intensity restriction.* The mathematical step of adiabatic elimination of all non- and near-resonant states is only reasonable as long as the population of these states is negligible. This leads to the detuning-dependent upper limit for the possible laser intensity, which is ~50 W/cm^2 for our chosen parameters. The ac Stark shift would require an intensity of $\sim10^5$ W/cm^2 to shift the Rydberg state into its neighbor state and thus does not restrict the laser intensity.

(b) *Time restriction.* The natural lifetime of the Rydberg state and the effective traveling time of the atomic beam across the laser beam both lead to an upper limit of ~1 μs for the reasonable time. Fortunately, this restricting time is 10 times larger than the dynamically necessary evolution time.

(c) *Laser linewidth restriction.* For colored chaotic light the linewidth must be smaller than the detuning in order to leave the state nonresonant and thus not violating the condition of adiabatic elimination. The usual available laser linewidths of 10 MHz to 100 GHz (10^{-8} a.u.) are all smaller than our detuning $\Delta=5\times10^{-7}$ a.u.

V. COLORED CHAOTIC LIGHT

The experimental verification of our theory would be performed with a multimode rather than a single-mode laser. Such a laser[12] should be described by a chaotic colored noise rather than deterministic amplitude $E(t)$. Assuming the simplest case of the Lorentzian spectrum, the second-order correlation function is

$$\langle E^*(t)E(t')\rangle = Ie^{-\Gamma_L|t-t'|}, \tag{5.1}$$

where I denotes the average laser intensity and Γ_L is the laser bandwidth. Of course, all the higher-order correlation functions obey the Gaussian decorrelation formula.

Our dynamical equations (2.5) in their general form allow us to write a solution in the form of a sum over eigenvalues λ_n for the tridiagonal matrix:

$$\alpha_j(t)=\sum_n C_n^j e^{i\lambda_n\eta(t)}. \tag{5.2}$$

Hence, the probabilities $P_j(t)=|\alpha_j(t)|^2$:

$$P_j(T)=\sum_{n,n'} C_n^{*j}C_{n'}^j \exp\left[i(\lambda_n-\lambda_{n'}^*)\int_0^t |E(\tau)|^2 d\tau\right]. \tag{5.3}$$

This last expression can be easily averaged over the chaotic colored noise using the formula first derived by Slepian:[13]

$$\langle P_j(t)\rangle=\sum_{n,n'} C_n^{*j}C_{n'}^j f(i(\lambda_n-\lambda_{n'}^*)I,\Gamma_L,t), \tag{5.4}$$

where

$$\left\langle \exp\left[\frac{\gamma}{I}\int_0^t |E(\tau)|^2 d\tau\right]\right\rangle = f(\gamma,\Gamma_L,t)=\frac{2}{(1+r/q)\exp[\Gamma_L t(q-1)]+(1-r/q)\exp[-\Gamma_L t(q+1)]} \tag{5.5}$$

and

$$r=1-\gamma/\Gamma_L,\quad q=(1-2\gamma/\Gamma_L)^{1/2}. \tag{5.6}$$

The expression (5.5) simplifies for both very small and very large Γ_L. For $\Gamma_L\to0$

$$\left\langle \exp\left[\frac{\gamma}{I}\int_0^t |E(\tau)|^2 d\tau\right]\right\rangle = \frac{1}{1-\gamma t} \tag{5.7}$$

while for $\Gamma_L\to\infty$

$$\left\langle \exp\left[\frac{\gamma}{I}\int_0^t |E(\tau)|^2 d\tau\right]\right\rangle = e^{\gamma t}. \tag{5.8}$$

TABLE I. Atomic parameters.

j	l	ReA_j	ImA_j	ReB_j	ImB_j
1	1	6.53×10^5	-1.29×10^3		
2	3	7.01×10^5	-1.17×10^3	2.64×10^5	-333
3	5	7.76×10^5	-9.39×10^2	1.56×10^5	-200
4	7	5.68×10^5	-5.23×10^2	5.93×10^4	-89
5	9	1.45×10^5	-1.87×10^2	8.55×10^3	-28
6	11	5.22×10^4	-4×10^1	-3.3×10^1	-6

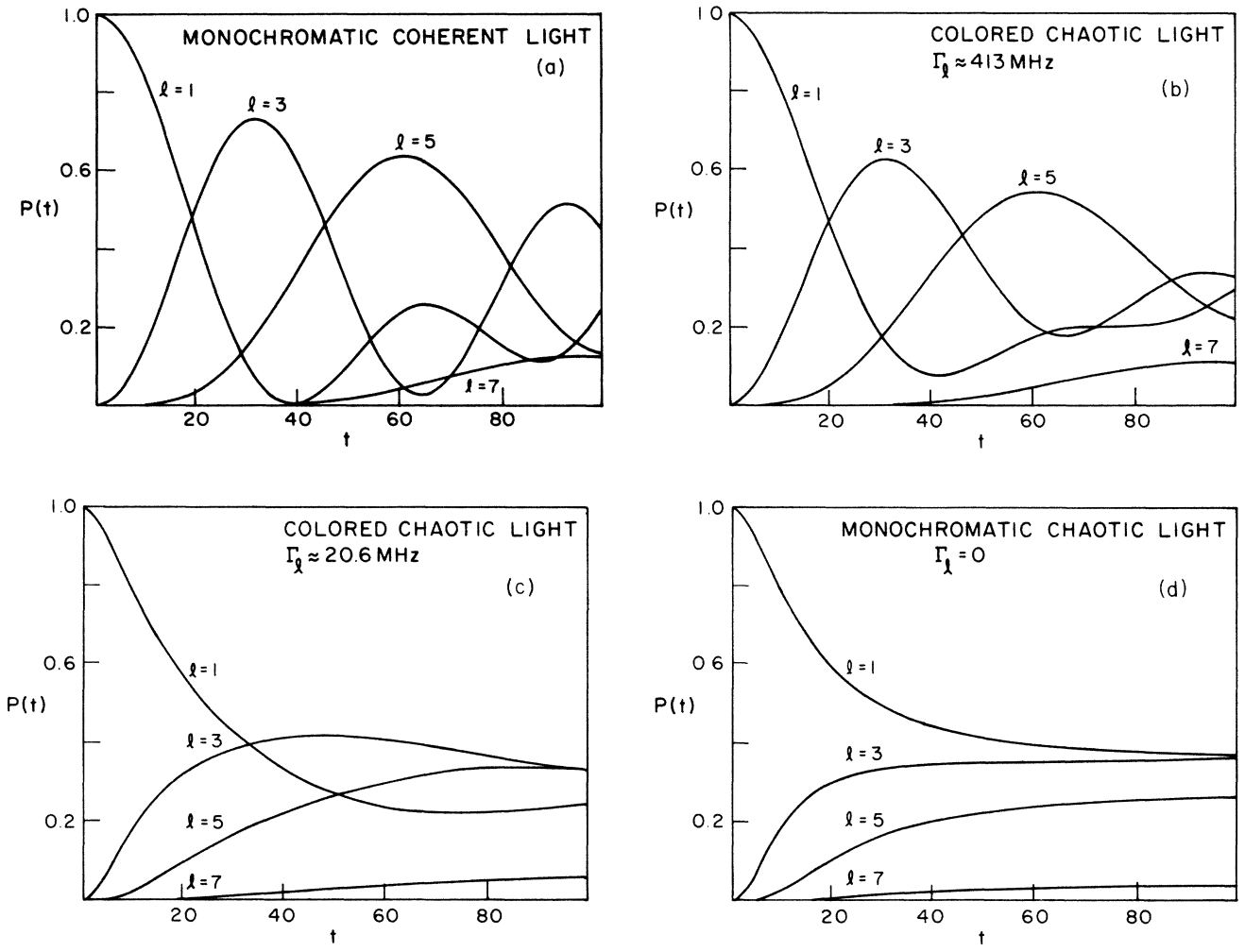

FIG. 3. The evolution of Rydberg states with principal quantum number $N=28$ and $l=1,3,5,7$ of hydrogen atom. Assumed laser frequency is that of CO_2 laser, intensity is 25 W/cm^2, time is in nanoseconds. The figures correspond to (a) coherent, monochromatic light, (b) chaotic colored light with $\Gamma_L=10^{-8}$ a.u. (413 MHz), (c) the same with $\Gamma_L=5\times10^{-10}$ a.u. (20.6 MHz), and (d) chaotic, monochromatic light.

This leads to a somewhat paradoxical result: A broadband chaotic laser acts on our atom in the same way as a monochromatic coherent laser, while a narrow-bandwidth chaotic laser produces strong effective suppression of the oscillations. This last point will be illustrated in Sec. VI. Of course, the average $\langle P_j(t)\rangle$ carries merely a small fraction of information about $P_j(t)$ as a stochastic variable. To shed some more light on this distribution we can easily compute its variance:

$$\Delta P_j=(\langle P_j^2\rangle-\langle P_j\rangle^2)^{1/2}\ . \tag{5.9}$$

The second moment, by the application of the same formula (5.5), is

$$\langle P_j^2\rangle=\sum_n\sum_{n'}\sum_{n''}\sum_{n'''}C_n^{*j}C_{n'}^{j}C_{n''}^{*j}C_{n'''}^{j}\times f(i(\lambda_n-\lambda_{n'}^*+\lambda_{n''}-\lambda_{n'''}^*)I,\Gamma_L,t) \tag{5.10}$$

and can be easily evaluated numerically.

Again, the broadband chaotic light produces the results that are the closest to a monochromatic coherent case. In fact

$$\lim_{\Gamma_L\to\infty}\langle P_j^2\rangle=\langle P_j\rangle^2\ . \tag{5.11}$$

VI. NUMERICAL RESULTS

In this section we present our main numerical results for the population migration in highly excited states of the hydrogen atom. Our procedure is very simple. First we compute all the couplings A_j and B_j for $N=28$ and the laser wavelength $\lambda_L=10\,445.5$ nm corresponding to a CO_2 laser. The results are summarized in Table I. The fast decrease of the Raman coupling with l is caused by the fact that the nearly resonant tenth level has $l_{\max}=9$

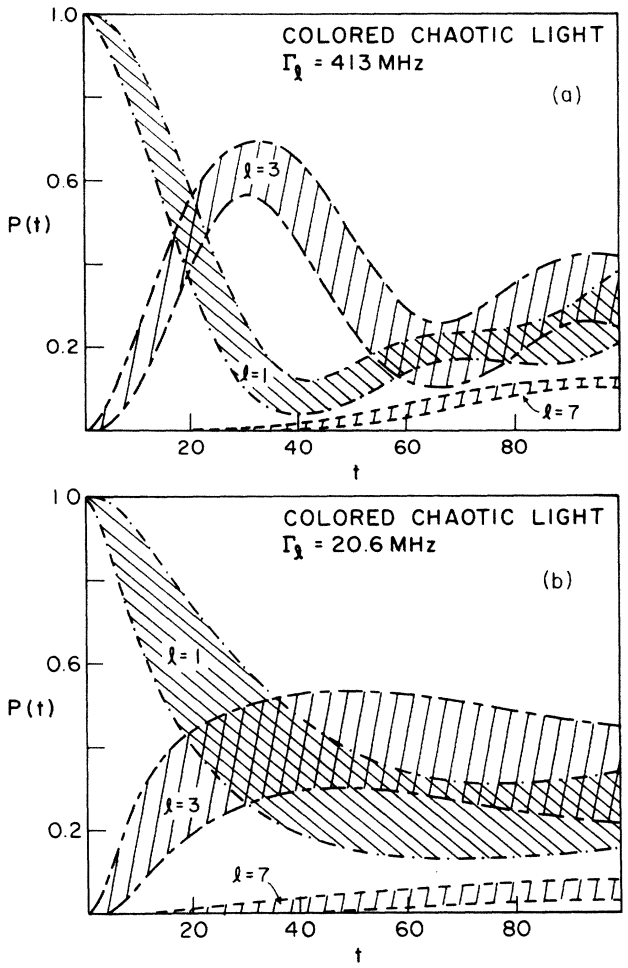

FIG. 4. Parameters are the same as Figs. 3(b) and 3(c). The fluctuations of $\langle P_j \rangle$ induced by the laser noise are explicitly marked. For clarity the evolution of the state with $l=5$ has been omitted.

and hence does not contribute to the transitions above $l=9$.

Given the laser intensity $I=25$ W/cm^2 and duration of the interaction $t=100$ ns the dynamics is well described by five-dimensional space. We find numerically all the eigenvalues, left- and right-hand-side eigenvectors (our matrix is non-Hermitian) and use the formula (5.4) to get the result for the chaotic colored noise.

The results are presented in Fig. 3. The population of the states with $l=1,3,5,7$ is plotted as a function of t for monochromatic coherent field (a), colored chaotic light with $\Gamma_L=10^{-8}$ a.u. (413 MHz) (b), and $\Gamma_L=5\times10^{-10}$ a.u. (20.6 MHz) (c), and for $\Gamma_L=0$ (d). The gradual suppression of oscillations is evident. For practical purposes chaotic colored light with $\Gamma_L=10^{-8}$ a.u. (413 MHz) behaves as monochromatic coherent, while chaotic colored light with $\Gamma_L=10^{-11}$ a.u. (0.4 MHz) behaves like chaotic light with $\Gamma_L=0$. It is clear that, depending on the kind of light used, we can expect 10—20 % of the population to migrate to the $l=7$ state.

The chaotic light induces a great deal of fluctuation. In Fig. 4 we have plotted P_1, P_3, and P_7 in the form of the strips: $\langle P_j \rangle \pm \frac{1}{2}\Delta P_j$ for two values of laser width: $\Gamma_L=10^{-8}$ and 5×10^{-10} a.u.. It is clear that fluctuations are maximum for the chaotic, very narrow bandwidth laser.

ACKNOWLEDGMENTS

We would like to thank our colleagues at the Joint Institute for Laboratory Astrophysics (JILA) for a fertile scientific atmosphere that all of us have enjoyed. One of us (R.G.) would like to thank the Fulbright Foundation for financial support and K.R. acknowledges support from the JILA Visiting Fellow Program.

*Permanent address: Fachbereich Physik, Universität Essen, D-4300 Essen, Essen 1, West Germany.

†Permanent address: Max Planck Institut für Quantenoptik, D-8046 Garching, West Germany.

‡Permanent address: Institute for Theoretical Physics, Polish Academy of Sciences, PL-02-668 Warsaw, Al. Lotników 32/46 Poland.

[1] *Multiphoton Processes,* edited by P. Lambropoulos and S. J. Smith, Vol. 2 of *Springer Series on Atoms and Plasmas* (Springer-Verlag, Berlin, 1984).

[2] P. Agostini and G. Petite, in Ref. 1, p. 13, and references therein.

[3] G. Leuchs, in Ref. 1, pp. 48—57; G. Leuchs, G. Alder, and S. J. Smith, Vol. 49 of *Springer Series in Optical Sciences* (Springer, Berlin, 1985).

[4] R. R. Freeman and D. Kleppner, Phys. Rev. A **14**, 1614 (1976).

[5] D. Kleppner, M. G. Littman and M. L. Zimmerman, in *Rydberg States of Atoms and Molecules,* edited by R. F. Stebbings and F. B. Dunning (Cambridge University, Cambridge, 1983).

[6] See, e.g., W. H. Louisell, *Quantum Statistical Properties of Radiation* (Wiley, New York, 1973), p. 288.

[7] Z. Białynicka-Birula, I. Białynicki-Birula, J. H. Eberly, and B. W. Shore, Phys. Rev. A **16**, 2048 (1977).

[8] W. Gordon, Ann. Phys. (Leipzig) **2**, 1031 (1929).

[9] This is a well-known Thomas-Reiche-Kuhn sum rule.

[10] P. Avan, C. Cohen-Tannoudji, J. Dupont-Roc, and C. Fabre, J. Phys. (Paris) **37**, 993 (1976).

[11] A similar relation between on- and off-diagonal two-photon matrix elements of low-lying states was recently discussed by B. Ritchie, Phys. Rev. A **30**, 1849 (1984).

[12] R. Loudon, *The Quantum Theory of Light* (Clarendon, Oxford, 1973).

[13] D. Slepian, Bell Syst. Tech. J. **37**, 165 (1958); see also P. Zoller and P. Lambropoulos, J. Phys. B **13**, 69 (1980).